

Coupled cluster calculations on TiO₂ nanoclusters.

Enrico Berardo¹, Hanshi Hu², Karol Kowalski^{2*}, Martijn A. Zwijnenburg^{1*}

¹*Department of Chemistry, University College London, 20 Gordon Street, WC1H 0AJ, UK.*

²*William R. Wiley Environmental Molecular Science Laboratory, Battelle, Pacific Northwest National Laboratory, K8-91, P.O. Box 999, Richland, Washington 99352, United States*

* *Corresponding authors email: karol.kowalski@pnnl.gov and m.zwijnenburg@ucl.ac.uk.*

The excitation energies of the four lowest-lying singlet excited states of the TiO₂, Ti₂O₄, and Ti₃O₆ clusters are calculated by a variety of different Equation-of-Motion Coupled Cluster (EOM-CC) approaches in order to obtain benchmark values for the optical excitations of titanium dioxide clusters. More specifically we investigate what the effect is of the inclusion of triple excitations “triples” in the (EOM-)CC scheme on the calculated excited states of the clusters. While for the monomer and dimer the inclusion of triples is found to only cause a rigid shift in the excitation energies, in the case of the trimer the crossing of the excited states is observed. Coupled cluster approaches where triples are treated perturbatively were found to offer no advantage over EOM-CCSD, whereas the active-space methods (EOM-CCSDt(II/I)) were demonstrated to yield results very close to full EOM-CCSDT, but at a much reduced computational cost.

1. Introduction

Understanding the excited state properties of Titania (TiO_2) and other transition metal oxide nanostructures (i.e. nanocluster, nanoparticles, nanotubes) and extended materials is extremely relevant and topical because of their importance in emerging technological applications such as photocatalytic watersplitting and dye-sensitized solar-cells. Transition metal oxides, however, are potentially challenging materials for standard computational chemistry and physics methods used to study the excited state properties of nanosized systems; Time-Dependent Density Functional Theory (TD-DFT) and Green's function methods (GW, GW_0), followed by solving the Bethe-Salpeter Equation (BSE). There is, therefore, a clear need for accurate correlated quantum chemistry benchmark calculations to compare the performance of methods such as TD-DFT and BSE with. Because of the computational scaling of accurate quantum chemistry methods such benchmark calculations by definition will focus on small clusters containing only one to three transition metal atoms and will purely concentrate on vertical excitation energies.

Ideally, the quantum chemistry method used for the benchmark calculations should yield results as close as possible to the exact solution of the electronic time-independent non-relativistic Schrödinger equation (or in practice a Full Configuration Interaction (FCI) calculation for the same basis-set). This means a method that describes all contributions to the electron correlation beyond the Fermi correlation (or exchange), correlation between the motion of electrons of the same spin, already included in the Hartree-Fock (HF) theory that underlies all quantum chemical methods. This means a method that ideally describes both *dynamic* (Coulomb) correlation, correlation between the motion of electrons independent of their spin that is absent from HF because of the mean-field approximation, and *static* correlation,

which arises from the inability of a single Slater determinant to describe situations where different electronic configurations (Slater determinants) lie close in energy, equally well. Moreover, the ideal method treats the electronic ground state and excited state on the same well-balanced footing and is unambiguously defined. In practice such an ideal method does not exist. FCI is prohibitively expensive for everything but atoms and very small molecules and all the other methods are primarily geared towards describing either dynamic (e.g., truncated Configuration Interaction¹, CI, or Coupled Cluster¹, CC, methods) or static (e.g., Complete Active Space Self Consistent Field², CASSCF, and other multiconfigurational-SCF based methods) electron correlation. Although, taking the above into account, CASSCF with a well-defined and well-balanced CAS (the active space of orbitals for which essentially a full CI is performed, typically consisting of 6-16 orbitals and containing 6-16 electrons) followed by a second-order perturbation step (combined in the CASPT2, Complete Active Space 2nd order Perturbation Theory^{3,4}) is likely to recover a large part of the *dynamical* correlation. Equally CCSDT⁵ (a Coupled Cluster calculation including Single, Double and Triple excitations) has been shown to recover, at least, part of the *static* correlation and to perform well for classic ground state *static* correlation problems such as the breaking of bonds.⁶ Finally, within the coupled cluster framework the ground state energy is calculated using a total energy approach while the excitation energy are obtained using an Equation-Of-Motion (EOM) formalism, while within, for example, CASSCF all states (including the ground state) are calculated variationally. The latter means that to guarantee orthogonality between states belonging to the same irreducible representation state-averaging has to be employed, where all such states are optimized together, and the results might become slightly dependent on the number of states studied.

Both CASSCF/CASPT2⁷ and CC^{7,8} (EOM-CCSD, i.e. EOM-CC theory with Single and Double excitations) have previously been used to study excitations for the TiO₂ monomer and found to yield very similar results. Use of more approximate methods (CIS, CIS(D), CC2) have also been reported in the literature but were found to give very unreliable results when compared with CASPT2 and EOM-CCSD.⁸ In this paper we focus on CC as for transition metal clusters it is not clear cut which orbitals and electrons to include in the active space and a strategy of simply including all valence electrons and orbitals is only tractable for the TiO₂ monomer (in part because of the 5 d-orbitals per titanium atom). We consider EOM-CCSD, EOM-CCSDT and a number of CC models that combine CCSD models with some approximate treatment of the triples, and predict spectra for the global minimum energy geometries⁹⁻¹⁸ (i.e., the most stable isomers) of not only the TiO₂ monomer but also the Ti₂O₄ dimer and the Ti₃O₆ trimer (see Figure 1). We specifically will discuss the effect of including triple excitations into CC (i.e., EOM-CCSDT) and the required balance between treating the triples contribution iteratively and/or approximating part of the triples contribution perturbatively. In the remainder of the paper we will first revisit CC theory and the different possible CC models (section 2), then discuss technical details of the practical calculations (section 3), followed by a discussion of the spectra obtained for the different clusters (sections 4 and 5) and conclusions.

2. Equation-of- Motion Coupled cluster methods

The Equation-of-motion coupled cluster theory (EOM-CC)¹⁹⁻²¹ can be viewed as an excited-state extension of single reference CC formalism, where the wavefunction of K-th state $|\Psi_K\rangle$ is obtained by acting with the state-specific excitation operator R_K onto an already correlated CC ground-state wavefunction; that is

$$|\Psi_K\rangle = R_K e^T |\Phi\rangle$$

In the above formula T is the cluster operator and $|\Phi\rangle$ is the reference function, usually chosen as a Hartree-Fock determinant. The T and R_K operators can be represented as sums of their many-body components T_i and $R_{K,i}$:

$$T = \sum_{i=1}^m T_i$$

$$R_K = \sum_{i=0}^m R_{K,i}$$

In our study of TiO₂ clusters we used several EOM-CC methods including EOM-CCSD ($m=2$),^{22,23} EOM-CCSDT (EOMCC with single, double, and triple excitations; $m=3$),²⁴⁻²⁶ and several variants of the active-space EOM-CCSDT approach (EOM-CCSDt)²⁷ where the selection of the most important triply excited excitations is made based on the active space concepts. More specifically, we employ the EOM-CCSDt(III)/ EOM-CCSDt(II)/ EOM-CCSDt(I) family of active space EOM-CC methods,²⁸ which include increasing subsets of triple excitations. For example, in the most rudimentary EOM-CCSDt(III) approach triply excited amplitudes carry active spinorbitals only (t_{ABC}^{IJK} and r_{ABC}^{IJK} , where upper case I, J, K, \dots (A, B, C, \dots) indices refer to the occupied (unoccupied) active spinorbitals). The EOM-CCSDt(II) and EOM-CCSDt(I) approaches use larger domain of triple excitations defined by (t_{ABC}^{ijk} , r_{ABC}^{ijk} ; lower case indices i, j, \dots (a, b, \dots) refer to generic occupied (unoccupied) indices) and (t_{Abc}^{ijk} , r_{Abc}^{ijk}) sets of triply excited cluster amplitudes, respectively. In addition to the iterative EOM-CC methods we also utilized various non-iterative completely renormalized EOM-CCSD(T) approach (CR-EOM-

CCSD(T))²⁹ and its reduced variant (r-CR-EOMCCSD(T) method of Ref. ³⁰) where the effect of triply excited configurations is accounted for in a perturbative manner. Although the EOM-CCSDT approach is capable of providing very accurate estimates of excitation energies for a wide class of excited states its applicability is limited by its steep numerical scaling proportional to N^8 , where N symbolically represents system-size. For this reason the EOM-CCSDT can be used in calculations for relatively small molecular systems. More details on the EOM-CC formulations can be found in several review papers.³¹

3. Computational details

The geometry of all the structures used in this work were optimized at the DFT level with the hybrid B3LYP³² exchange-correlation (XC) functional in conjunction with the triple- ζ def2-TZVP basis set.³³ The Harmonic frequencies at these optimized geometries were calculated employing the same DFT setup to verify that the optimized structures correspond to proper minima on the ground state potential energy surface. Use of the B3LYP optimized ground state structure instead of a CCSD/CCSDT optimized structure was found to introduce differences in the calculated excitation energies of less than 0.05 eV in case of the monomer, and is the only realistic alternative for larger clusters.

The electronic ground state of all the clusters studied in this work is a closed-shell singlet. The optimized structure for the monomer (TiO₂) has a C_{2v} geometry with Ti-O bond length (1.641 Å) and O-Ti-O bond angle (111.8°) in good agreement with the accurate multireference-CI³⁴ (MRCI) results obtained by Grein,³⁵ which showed a bond length of 1.640 Å and O-Ti-O bond angle of 112.0° respectively. The optimized structure for the lowest energy dimer (Ti₂O₄) has a C_{2h} geometry with O-Ti (terminal bonds) bond lengths of 1.627 Å and Ti-O bond lengths of 1.847 Å, which compares

well with the minimum energy geometry found by Li and Dixon at the CCSD(T) level¹² with bond lengths of 1.648 Å and 1.863 Å respectively. A large set of other dimer structures is known, where two of them lie relatively close in energy to the global minimum.^{9,36,37} These two structures, with C_{2v} and C_s symmetry respectively, lie 0.25 and 0.73 eV higher in energy than the lowest energy dimer (B3LYP), and are not considered here. The optimized trimer structure (Ti_3O_6) with two terminal and one 3-fold coordinated oxygen atom, has C_s symmetry and it is in agreement with the global minimum obtained in previous studies at B3LYP level.^{10-14,16-18,37} Previous studies located on the trimer energy landscape a multitude of higher lying isomers, with a series of different coordination environments for the titanium and oxygen atoms. Among this set, the lowest energy alternative trimer structure (also with C_s symmetry) has two terminal oxygen atoms, a three-fold coordinated titanium atoms and lies 0.36 eV higher in energy (B3LYP).³⁷ Again, its excitations are not studied here. Please find the B3LYP optimized Cartesian coordinates for the respective global minima cluster in the ESI.³⁸

The singlet vertical excitation energies of the four lowest-lying excited states for the DFT ground state geometries have been calculated with various variants of coupled cluster theory including EOM-CCSD, CR-EOM-CCSD(T), r-CR-OM-CCSD(T), EOM-CCSDT and different versions of active-space EOM-CCSDt (I/ II/ III). More information about the different coupled cluster approaches can be found in the introduction. The most expensive EOM-CCSDT calculations for the trimer molecule have been performed using 2.000 cores on the Olympus cluster (Atipa Cluster, Opteron 6272 16C 2.100GHz, Infiniband QDR) at the Pacific Northwest National Laboratory. To calculate adiabatic excitation energies in the case of the monomer relevant excited states were relaxed using EOM-CCSD, while keeping the point group

symmetry fixed, followed in the case of EOM-CCSDT by a EOM-CCSDT single-point vertical excited state calculation on the EOM-CCSD optimized geometry.

The performance of the EOM-CC methods has been tested for a series of different basis sets. The selected basis sets are the small split-valence def2-SV(P) basis-set³⁹ and the larger triple- ζ def2-TZVPP basis set,³³ which from now on will be defined as SV and TZ respectively. Moreover, for selected systems we have also used a triple- ζ aug-cc-pVTZ⁴⁰ basis set to compare with literature results (further referred to as ATZ). The majority of the coupled cluster calculations, for reasons of computational tractability, employed the frozen core approximation, where only the valence electrons are correlated (i.e, the 1s orbitals of the oxygen atoms and the 1s to 3p orbitals of the titanium atoms are frozen in the CC calculations). However, for the smallest structure in this work (TiO₂) we were able to obtain the vertical excitation at the EOM-CCSD level of theory, employing the def2-TZVPP and the aug-cc-pVTZ all electron approach, which from now on will be referred to as aeTZ and aeATZ respectively. The electronic character of the excitations found by CC methods is interpreted in terms of the single and double electron orbital excitations with the largest EOM-CC amplitudes (R_1 and R_2), where we deem amplitudes as significant when $R_n > 0.1$ and a leading contribution for $R_n > 0.25$. The largest EOM-CC amplitudes are reported in specific R-vector normalization employed by the EOM-CC eigensolver.

The DFT ground state calculations, finally, were performed with the Turbomole 6.4 code,⁴¹ while all the coupled cluster calculations employed the Tensor Contraction Engine (TCE) module⁴² of the NWChem 6.1 package.⁴³

4. Results and discussion

We will now review the excitation energies for the three clusters calculated with the different method combinations and then discuss the role of including triples and the practical balance between including triples and the quality of basis-sets one can employ.

4.1 Monomer

Figure 2 shows the four lowest excitation energies for the TiO_2 monomer cluster (please see the ESI for matching tables with excitation energies).³⁸ As can be seen all method combinations (except for the all-electron SV EOM-CCSD calculation) find the same ordering of excited states and relative gaps (i.e., a large gap between S_1 and S_2 , i.e. 1^1B_2 and 1^1A_2 , and smaller gaps between S_2 and S_3 and S_3 and S_4). Increasing the basis-set quality from the split-valence SV basis-set to the larger triple- ζ zeta TZ basis-set is found to result in a consistent upward shift in the calculated excitation energies of ~ 0.2 eV, while going from the frozen core approximation to an all electron calculation, where feasible, results in a consistent downward shift in the calculated excitation energies of ~ 0.1 eV. Including triples iteratively using EOM-CCSDt(I) and EOM-CCSDT leads to a consistent down-ward shift of up to ~ 0.25 eV. EOM-CCSDt(III/II) yields excitation energies in between those calculated with EOM-CCSD and EOM-CCSDT, while EOM-CCSDt(I) slightly overshoots and predicts values that are slightly lower than those obtained with EOM-CCSDT. The non-iterative perturbative triples CR-EOM-CCSD(T) method, finally, yields results that lie ~ 0.1 eV above the values obtained with plain EOM-CCSD. A similar thing happens for EOM-CCSDt(III/II) (EOM-CCSDt(III) results in the ESI),³⁸ the active space methods with the smaller subset of triple excitations employed (see Section 2), which yield values close to those obtained with EOM-CCSD.

The EOM-CCSD aeTZ data from Figure 2 (and the EOM-CCSD aeATZ data given in the ESI)³⁸ agree very well with EOM-CCSD, CASPT2 and MRCI results from the literature. The difference with the literature EOM-CCSD data is consistently smaller than 0.06 eV, the differences with the published CASPT2 data is smaller than 0.1 eV for the lowest two excitations and less than 0.2 eV for the next two, while the difference with the literature MRCI data is smaller than 0.05 eV for all but the a1 excitation. While we did not run EOM-CCSDT aeTZ calculations for all irreducible representations due to the computational cost involved with such calculations, aeTZ EOM-CCSDT results for the lowest 1B_2 excitation (2.12 eV) show a 0.14 eV further downward shift when going from the frozen-core approximation to including all-electrons, in-line with what is observed for EOM-CCSD/aeTZ, EOM-CCSD/aeATZ, and EOM-CCSDT/aeSV. The EOM-CCSDT aeTZ for the 1B_2 state (and the other states by extrapolation) thus lies ~ 0.3 eV lower than the corresponding states found with CASPT2 and MRCI.

Comparison with experimental spectral data for the TiO_2 molecule is complicated as typically adiabatic rather than vertical excitation energies are reported.⁴⁴⁻⁴⁶ The most recent experimental study on molecular beams of TiO_2 molecules reports an adiabatic excitation energy of 2.18 eV⁴⁶ for a state identified, partly based also on previous computational work, as the 1B_2 state. Previous experimental work on TiO_2 in a neon solid matrix⁴⁴ also yielded another adiabatic excitation energy at 1.97 eV (together with what was identified as the 1B_2 excitation at 2.37 eV, slightly higher than in the molecular beam experiment). This 1.97 eV adiabatic excitation was assumed to originate from a linear isomer of the monomer instead of the global minimum bent C_{2v} isomer studied here, because none of the computational studies performed till that date had predicted any excitation energies lower than 2.4 eV. Finally, the authors of

the more recent molecular beam experiments report not seeing the 1.97 eV adiabatic excitation (but do not show the relevant spectral range in the paper), which they argue is due to the fact that the linear isomer is a higher energy isomer that might not be created in the laser ablation process used to prepare the TiO₂ clusters for their molecular beam.

To compare our results with experiment we optimized the lowest two (i.e. 1^1B_2 and 1^1A_2) excited states using EOM-CCSD, followed by single-point EOM-CCSDT calculations where possible, and calculated the adiabatic excitation energies. Just as in previous work we observe that for the 1^1B_2 state optimization results in a decrease of the O-Ti-O angle to $\sim 101^\circ$ (see ESI for CCSD optimized geometry),³⁸ while the optimized 1^1A_2 geometry becomes effectively linear (O-Ti-O angle to $\sim 180^\circ$), where the exact angle depends on the specific basis-set used. Table 1 gives the as such calculated adiabatic excitation energies. Focusing on the larger basis-set results (i.e. TZ and ATZ) it is clear that EOM-CCSD yields a 1^1B_2 adiabatic excitation energy that lies relatively close (< 0.2 eV) to the value measured in the molecular beam experiment, especially when including the core-electrons in the EOM-CCSD calculations (i.e. using aeTZ and aeATZ basis-sets). This fits with the previous computational work of Lin *et al*⁷ who made a similar observation for their EOM-CCSD calculations. The EOM-CCSDT calculations yield values that lie further away from experiment (below instead of above). Specifically, an all electron EOM-CCSDT calculation with the aeTZ basis-set yields a 1^1B_2 adiabatic excitation energy of 1.92 eV (2.01 eV with the frozen-core approximation). However, it is tantalizing to note that this 1.92 eV value lies very close to the 1.97 eV value measured in the neon matrix. One could suppose that the 2.18 eV peak then finds its origin in an adiabatic excitation into a higher excited state of the monomer (e.g. 2^1B_2 and 2^1A_1). While we

find that the 1^1A_2 state lies in the correct range it would make an unlikely candidate for the 2.18 eV adiabatic excitation in this scenario, as an $1A_2$ excitation is symmetry forbidden (at least in the case of vertical excitations at both the ground state and relaxed excited state geometries) and hence would have low intensity. Most importantly, our calculations suggest that the original identification of the 1.97 eV adiabatic excitation as originating from a linear isomer might need to be revisited.

The leading single electron HF excitation contributions to the lowest 1^1B_2 excitation for both EOM-CCSD and EOM-CCSDT are HOMO \rightarrow LUMO and HOMO \rightarrow LUMO+2 ($R_1 > 0.25$). In all cases the relevant occupied orbital involve p-orbitals on the terminal oxygen atoms, while the unoccupied virtual orbitals are d-like orbitals located on the central titanium atom (see ESI)³⁸. There are no significant double electron HF excitation contributions ($R_2 > 0.1$).

4.2 Dimer

Figure 3 shows the four lowest excitation energies for the trans Ti_2O_4 dimer cluster. Just as for the monomer all method combinations find the same ordering of excited states and relative gaps, the effect of increasing the basis-set from SV to the triple- ζ zeta TZ is an upward shift of ~ 0.2 eV, and the effect of including perturbative triples is ~ 0.3 eV (slightly larger than for the monomer). CR-EOM-CCSD(T) does slightly better than for the monomer but still does not seem to improve beyond EOM-CCSD. Finally, all methods predict the excitation energies for the dimer to consistently lie higher in energy than their monomer counterparts (by ~ 1.4 eV for the lowest excitation and ~ 0.8 eV for all the others).

The leading single electron HF excitation contributions to the lowest energy 1^1B_g excitation for both EOM-CCSD and EOM-CCSDT are HOMO \rightarrow LUMO, HOMO \rightarrow

LUMO+3, HOMO-1 \rightarrow LUMO+1 (See ESI).³⁸ In all cases the relevant occupied orbital involve p-orbitals on both the terminal and two-fold coordinated oxygen atoms, while the virtual orbitals are predominantly localized on the two titanium atoms (see ESI).³⁸ Just as for the monomer there are no significant double electron HF excitation contributions.

4.3 Trimer

Figure 4 shows the four lowest (two lowest for EOM-CCSDT, where fully converging two excitations per irreducible representation was found to be numerically intractable) excitation energies calculated for the Ti_3O_6 trimer cluster. Here, in contrast to the monomer and dimer, do we see a clear effect of including triples beyond a simple downward shift in energy. The lowest two excitations change ordering upon including a certain amount of perturbative triples. For EOM-CCSD, CR-EOM-CCSD(T) and EOM-CCSDt(III) the lowest singlet excitation has A'' symmetry, while for EOM-CCSDt(II), EOM-CCSDt(I) and EOM-CCSDT the lowest singlet root has A' symmetry. A similar switch can also be observed for the second pair of excitations. The fact that we see the switch in EOM-CCSDt(II), EOM-CCSDt(I) and EOM-CCSDT, where we could converge multiple excitations for the former methods, makes us feel comfortable that the observed switch is real and not an artifact resulting from the iterative solver missing the lowest lying excitation.

The position of the trimer excitations relative to those of the monomer and dimer are less sensitive to the inclusion or not of perturbative triples. All methods consistently predict that the lowest trimer excitation lies ~ 1.4 eV higher in energy than its monomer counterpart and is similar in energy to the lowest excitation of the dimer (slightly higher for EOM-CCSD and slightly lower for EOM-CCSDT).

The leading single electron HF excitation contributions to the lowest energy $2^1A'$ excitation for EOM-CCSD and EOM-CCSDT are HOMO \rightarrow LUMO, HOMO \rightarrow LUMO+2 and HOMO \rightarrow LUMO+8. As can be seen in Fig. 5 the occupied orbitals in these excitations are typically localized on the terminal oxygen atoms, while the virtual orbitals are predominantly localized on the triply coordinated titanium atom. The main contributions to the lowest energy $1^1A''$ orbital are both in the case of EOM-CCSD and EOM-CCSDT HOMO-7 \rightarrow LUMO and HOMO-7 \rightarrow LUMO+2. The virtual orbitals are again localized on the three-fold coordinated titanium atom but the occupied orbitals are predominantly localized on the three oxygen atoms located around the three-fold coordinated titanium atom instead of the terminal oxygen atoms. The $1^1A''$ excitation thus appears more localized while the $2^1A'$ excitation has more long-distance charge-transfer character. Just as for the monomer and dimer, finally, there are no significant double electron HF excitation contributions for either the lowest $2^1A'$ and $1^1A''$ excitations.

4.4 Discussion

When considering the effect of including triples in coupled cluster calculations two different but interrelated effects have to be distinguished; (i) a (rigid) shift in excitation energies and (ii) crossing of excited state energies. All three clusters studied here show a non-negligible type (i) effect, where the EOM-CCSDT excitation energies are invariably located 0.3-0.4 eV below the EOM-CCSD excitation energies. For the trimer also a type (ii) effect was observed, where the $1^1A''$ and $2^1A'$ states cross when going from EOM-CCSD to EOM-CCSDT, while for the monomer and dimer excited states were not found to cross. The lowest excited states for all clusters are dominated by single-electron excitations (see above) so it is unlikely that effect (i) and (ii) are related to excitations having double excitation character, and hence their

origin must lie in an improved description of *static* (and *dynamic*) correlation. The rigid shift (i) might be ironically related to an improved description of the ground state in the CCSDT calculation that precedes the EOM-CCSDT excited state calculation. This might also explain why methods based on non-iterative triples (e.g. CR-EOM-CCSD(T)) do not yield improved results relative to EOM-CCSD. Such methods add triples corrections to the excited state but describe the ground state with standard CCSD. The exact origin of the crossing of states for the trimer is also unknown but it might be related to the fact that, as outlined above, the $2^1A'$ and $1^1A''$ excitations have a fundamentally different chemical character, while for the monomer and dimer all lowest excited states have a similar character. Another contributing fact might be that, as can be seen in Fig. 6, the spectrum of Hartree-Fock orbitals that enter the EOM-CC calculation becomes denser with increasing cluster size and unoccupied orbitals end up lying increasingly close in energy. It is also of note that the lowest singlet $2^1A'$ excitation for the trimer is an extreme case in terms of the number of the significant amplitudes ($R_1 > 0.1$) changing when going from EOM-CCSD to EOM-CCSDT. For the lowest $2^1A'$ excitation of the trimer the number of significant amplitudes changes from 10 to 3 (i.e. seven amplitudes decrease to a $R_1 < 0.1$), while the number of significant amplitudes for the lowest $1^1A''$ excitation stay constant and the observed difference for the lowest excitations of the other clusters is at most a reduction of two. The 0.1 cut-off is to a certain extent arbitrarily but the large change for the $2^1A'$ excitation and lack of change for the $1^1A''$ excitation respectively, suggests that the origin of the state crossing is a different description of the states in EOM-CCSD and EOM-CCSDT. This is, finally, corroborated by the fact that for the lowest $2^1A'$ trimer excitation, the largest amplitude changes when going from EOM-CCSD to EOM-CCSDT (from HOMO \rightarrow LUMO+8 to HOMO \rightarrow LUMO,

see Fig. 5), again something not observed for the other clusters or the lowest $1^1A''$ excited state of the trimer.

The computational cost of EOM-CCSDT relative to EOM-CCSD (N^8 vs. N^6 scaling) is found to be a practical constraint on the size of systems that can be studied and/or the size of basis-sets that can be employed. Specifically, in the case of the monomer EOM-CCSDT calculations with the triple- ζ TZ and aeTZ basis sets were found to be feasible on contemporary parallel machines while for the larger clusters only EOM-CCSDT calculations with the smaller SV basis-set were found to be tractable. For example, for the monomer and using 120 cores in each case, a single EOM-CCSD/SV iteration for 3 roots per irreducible representation took 2-7 seconds, a single EOM-CCSDT/SV iteration 30-90 seconds and a single EOM-CCSDT/TZ iteration 2300-2600 seconds. For the trimer a single EOM-CCSDT/SV iteration took around 1200-1500 seconds, when 2048 cores were employed in the calculation with five gigabytes of memory per core. There is thus, currently at least, for the dimer and trimer a tradeoff between improving the method (i.e. including triples) and maintaining the quality of the basis-set (i.e. the need to reduce the basis-set from TZ to SV). The EOM-CCSDt(I) active-space method was found to yield results that are very close to full EOM-CCSDT at a lower computational cost. However, while use of EOM-CCSDt(I) generally allowed more roots to be studied than where feasible with EOM-CCSDT, the computational savings were typically not sufficient to allow the usage of a larger basis-set. EOM-CCSDT and EOM-CCSDt(I) calculations for clusters larger than the trimer were found to be currently numerically intractable. Coupled cluster approaches where triples are treated perturbatively (e.g. CR-EOM-CCSD(T)), while displaying advantageous scaling compared to EOM-CCSDT and EOM-CCSDt(I), were found to offer no advantage over EOM-CCSD and sometimes even found to

produce worse result. EOM-CCSD is thus the only feasible coupled cluster approach for systems that are too large to treat with either EOM-CCSDT or EOM-CCSDt(I). Our calculations suggest that when type (i) effects dominate an approximate idea of the possible EOM-CCSDT spectrum might be obtained by pragmatically shifting the EOM-CCSD spectrum by a rigid amount.

Finally, focusing on the chemistry rather than methodology, our calculations suggests that, independently of the exact method used, there is a distinct upward shift in excitation energies when going from the monomer to the dimer and trimer. The lowest energy excitations of the dimer and trimer are predicted to lie more than 1 eV higher in energy than that of the monomer. A tentative explanation for this difference in lowest excitation energy might lie in the oxygen coordination of the titanium atoms in the different clusters (two-fold in the monomer, three-fold in the dimer, and three/four-fold for the trimer) and hence the electrostatic field experienced by the excited electrons localized on the titanium atoms.

5. Conclusions

In this paper we studied the application of coupled cluster methods to study the optical excitations of TiO_2 clusters containing one to three Titanium atoms. We specifically focused on EOM-CC methods that included contributions of triples including full EOM-CCSDT, the approximate iterative active-space EOM-CCSDt(I) method and approaches that treat triples perturbatively; e.g. CR-EOM-CCSD(T). Our calculations show that there is a non-negligible effect of adding triples, mostly in the form of a downward shift in excitation energies relative to those obtained by EOM-CCSD, and that the approximate iterative active-space EOM-CCSDt(I) method yields results that are in good agreement with full EOM-CCSDT. Methods that treat triples

perturbatively in contrast are found to yield results that are not better of even worse than those obtained by EOM-CCSD. Finally, we find that for the larger clusters there is a tradeoff between method and basis-set, where calculations using methods that include iterative triples are currently only feasible with moderately-sized basis-sets.

6. Acknowledgements

We kindly acknowledge Drs. M. Calatayud, A. Kerridge, S. Shevlin, and S.M. Woodley for stimulating discussion. M.A.Z. acknowledges the UK Engineering and Physical Sciences Research Council (EPSRC) for a Career Acceleration Fellowship (Grant EP/I004424/1). This study has further been supported by a UCL Impact studentship award to EB. Computational time on the computers of the Unity High Performance Computing Facility at University College London, the IRIDIS regional high-performance computing service provided by the e-Infrastructure South Centre for Innovation (EPSRC Grants EP/K000144/1 and EP/K000136/1) and on HECToR the UK's national high-performance computing service (via our membership of the UK's HPC Materials Chemistry Consortium, which is funded by EPSRC grant EP/F067496) is gratefully acknowledged. A significant portion of the research was also performed using PNNL Institutional Computing at Pacific Northwest National Laboratory and EMSL, a national scientific user facility sponsored by the Department of Energy's Office of Biological and Environmental Research and located at Pacific Northwest National Laboratory. The Pacific Northwest National Laboratory is operated for the U.S. Department of Energy by the Battelle Memorial Institute under Contract DEAC06.76RLO-1830.

Fig. 1 Structures of the three $(\text{TiO}_2)_n$ global minima for $n = 1 - 3$.

Fig. 2 Trend in the four lowest excitation energies of the TiO_2 monomer as calculated with different method combinations (1^1B_2 red-line, 1^1A_2 green-line, 2^1B_2 blue-line, and 2^1A_1 purple-line; B_2 and B_1 labels interchanged to yield labels consistent with previous theoretical studies).

Fig. 3 Trend in the four lowest excitation energies of the Ti_2O_4 trans dimer as calculated with different method combinations (1^1B_g red-line, 1^1A_u green-line, 1^1B_u blue-line, and 2^1A_g purple-line).

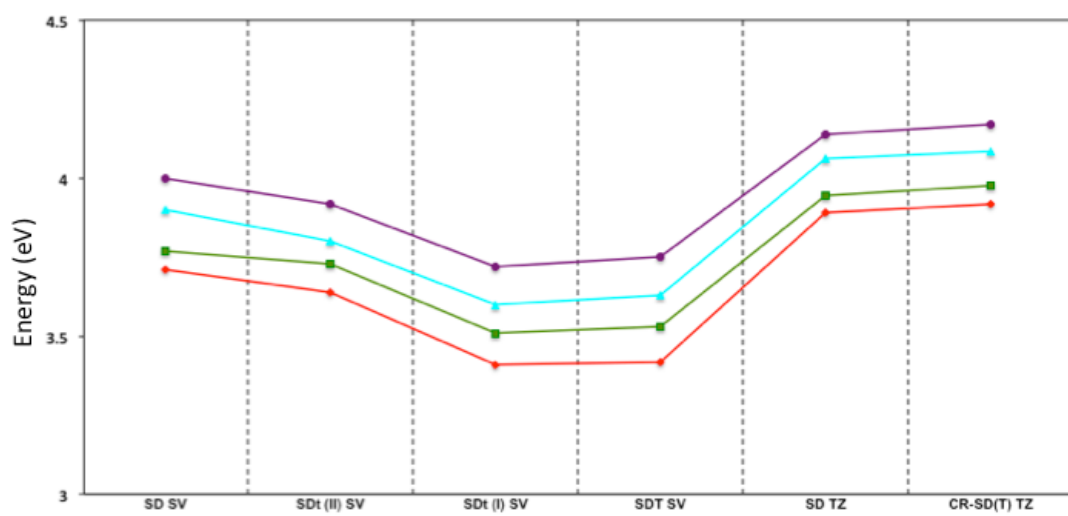
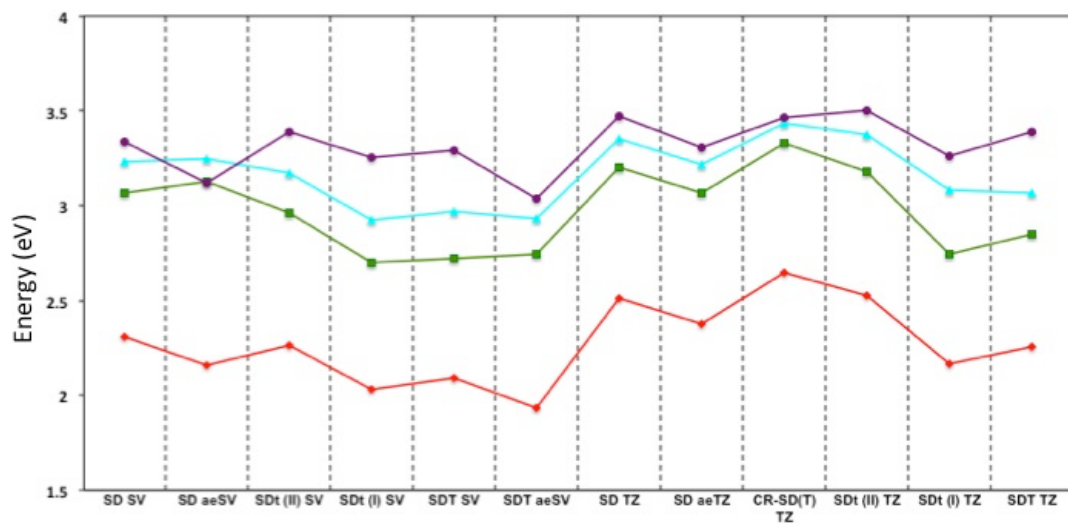
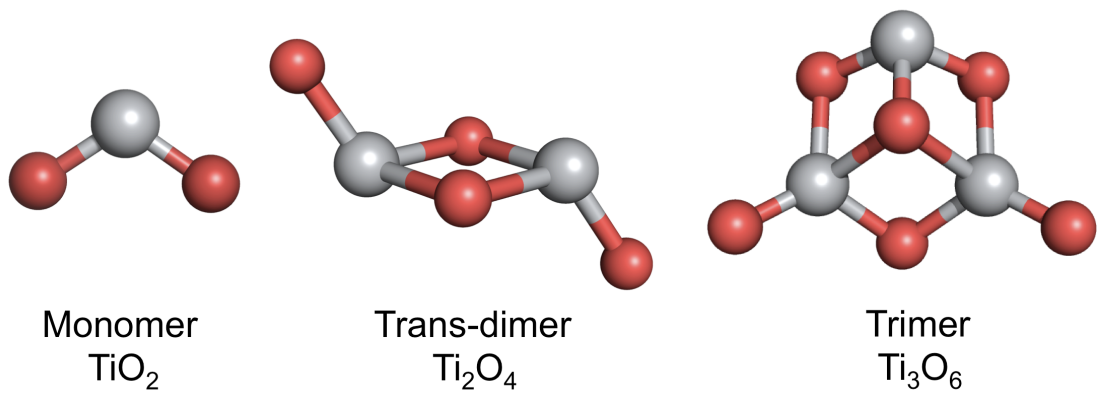
Fig. 4 Trend in the four lowest excitation energies of the Ti_3O_6 trimer as calculated with different method combinations ($2^1\text{A}'$ green-line, $1^1\text{A}''$ red-line, $2^1\text{A}''$ blue-line, and $3^1\text{A}'$ purple-line).

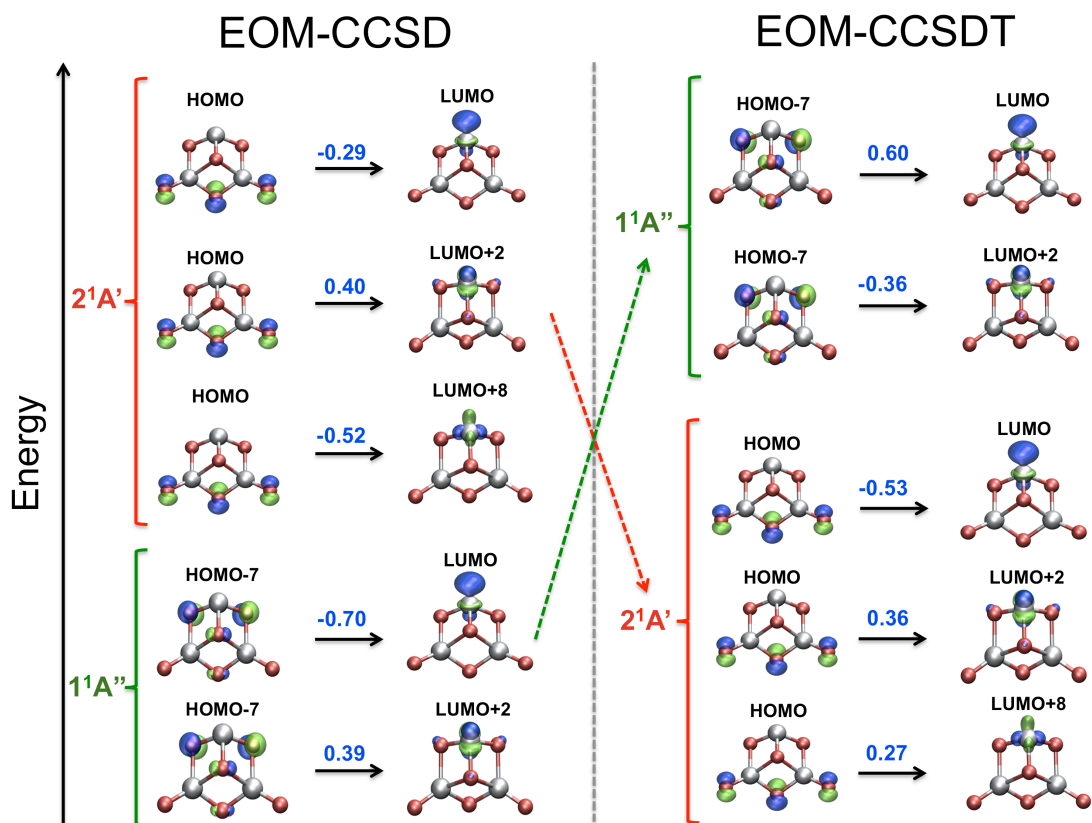
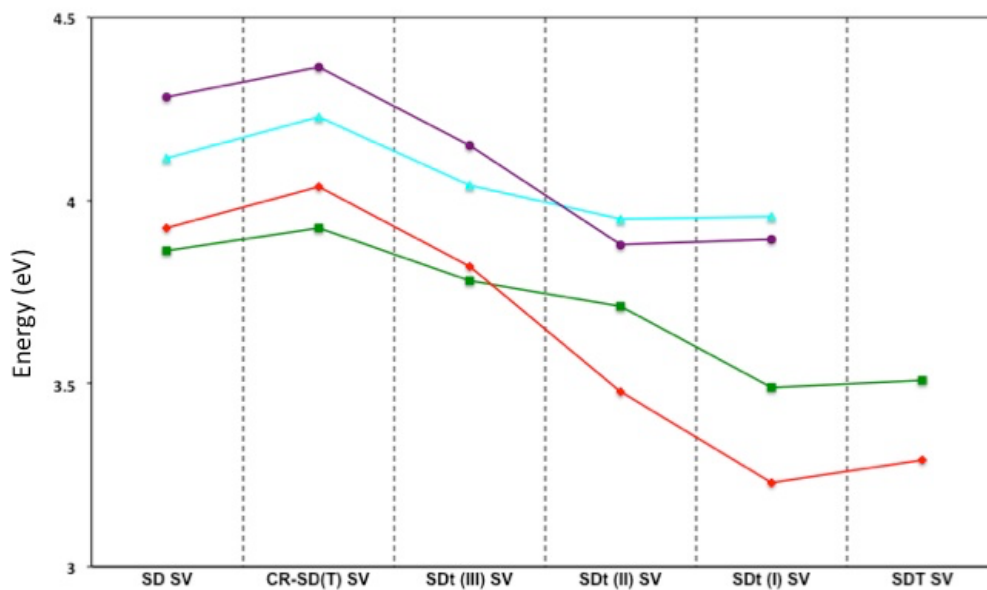
Fig. 5 Leading single electron HF excitation contributions ($R_1 > 0.25$) to the two lowest energy singlet A' and A'' excitations for the trimer, calculated with EOM-CCSD and EOM-CCSDT. For each contribution the amplitude value is specified in blue. The isodensity plots for the HF orbitals are calculated at a value of 0.1 a.u., where the green lobes represent the positive portion of the wavefunction and the blue orbitals correspond to the negative one.

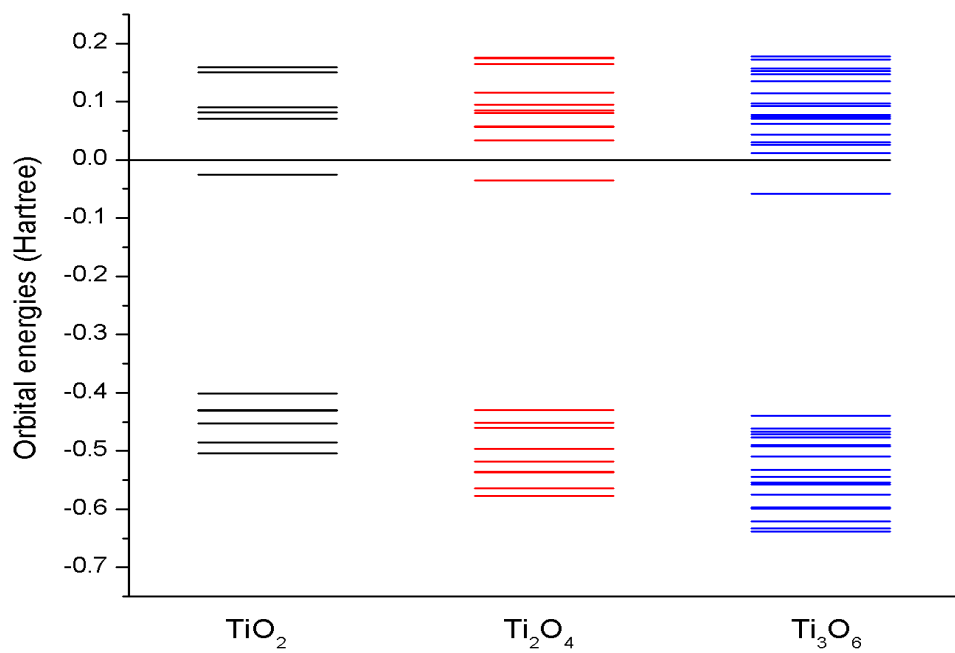
Fig. 6 Energy ordering of the HF orbitals (occupied and virtuals) for the TiO_2 monomer (black lines), Ti_2O_4 dimer (red lines) and Ti_3O_6 trimer (blue lines). All the energies are in Hartrees.

Table 1 Adiabatic excitation energies for the first and second excited state of the monomer as calculated with EOM-CCSD and EOM-CCSDT (single points on EOM-

CCSD optimised geometries, only where tractable) with the SV, TZ and ATZ basis-sets (all electron results, where tractable, given between parentheses).







		SV	TZ	ATZ
1^1B_1	EOM-CCSD	2.21 (2.11)	2.42 (2.32)	2.45 (2.35)
	EOM-CCSDT	1.80 (1.73)	2.01 (1.92)	---
1^1A_2	EOM-CCSD	2.43	2.64 (2.48)	2.64 (2.47)
	EOM-CCSDT	2.05	2.32	---

References

- (1) Szabo, A.; Ostlund, N. S. *Modern quantum chemistry, introduction to advanced electronic structure theory*; McGraw-Hill, Inc.: New York, 1989; Vol. 1982.
- (2) Roos, B. O.; Taylor, P. R.; Siegbahn, P. E. M. *Chem. Phys.* **1980**, *48*, 157.
- (3) Andersson, K.; Malmqvist, P. A.; Roos, B. O.; Sadlej, A. J.; Wolinski, K. *J. Phys. Chem.* **1990**, *94*, 5483.
- (4) Andersson, K.; Malmqvist, P. A.; Roos, B. O. *J. Phys. Chem.* **1992**, *96*, 1218.
- (5) Noga, J.; Bartlett, R. J. *J. Chem. Phys.* **1987**, *86*, 7041.
- (6) Yang, K. R.; Jalan, A.; Green, W. H.; Truhlar, D. G. *J. Chem. Theory Comput.* **2012**, *9*, 418.
- (7) Lin, C.-K.; Li, J.; Tu, Z.; Li, X.; Hayashi, M.; Lin, S. H. *Rsc Advances* **2011**, *1*, 1228.
- (8) Taylor, D. J.; Paterson, M. J. *J. Chem. Phys.* **2010**, *133*.
- (9) Hamad, S.; Catlow, C. R. A.; Woodley, S. M.; Lago, S.; Mejias, J. A. *J. Phys. Chem. B* **2005**, *109*, 15741.
- (10) Qu, Z. W.; Kroes, G. J. *J. Phys. Chem. B* **2006**, *110*, 8998.
- (11) Calatayud, M.; Maldonado, L.; Minot, C. *J. Phys. Chem. C* **2008**, *112*, 16087.
- (12) Li, S.; Dixon, D. A. *J. Phys. Chem. A* **2008**, *112*, 6646.
- (13) Liu, Y.; Yuan, Y.; Wang, Z.; Deng, K.; Xiao, C.; Li, Q. *J. Chem. Phys.* **2009**, *130*, 174308.
- (14) Shevlin, S. A.; Woodley, S. M. *J. Phys. Chem. C* **2010**, *114*, 17333.
- (15) Chiodo, L.; Salazar, M.; Romero, A. H.; Laricchia, S.; Della Sala, F.; Rubio, A. *J. Phys. Chem.* **2011**, *135*, 244704.
- (16) Syzgantseva, O. A.; Gonzalez-Navarrete, P.; Calatayud, M.; Bromley, S.; Minot, C. *J. Phys. Chem. C* **2011**, *115*, 15890.
- (17) Marom, N.; Kim, M.; Chelikowsky, J. R. *Phys. Rev. Lett.* **2012**, *108*, 106801.
- (18) Taylor, D. J.; Paterson, M. J. *Chem. Phys.* **2012**, *408*, 1.
- (19) Comeau, D. C.; Bartlett, R. J. *Chem. Phys. Lett.* **1993**, *207*, 414.
- (20) Geertsen, J.; Rittby, M.; Bartlett, R. J. *Chem. Phys. Lett.* **1989**, *164*, 57.
- (21) Stanton, J. F.; Bartlett, R. J. *J. Chem. Phys.* **1993**, *98*, 7029.
- (22) Koch, H.; Jorgensen, P. *J. Chem. Phys.* **1990**, *93*, 3333.
- (23) Monkhorst, H. J. *International Journal of Quantum Chemistry* **1977**, 421.
- (24) Nakatsuji, H.; Hirao, K. *Chem. Phys. Lett.* **1977**, *47*, 569.
- (25) Nakatsuji, H.; Hirao, K. *J. Chem. Phys.* **1978**, *68*, 2053.
- (26) Nakatsuji, H.; Hirao, K. *J. Chem. Phys.* **1978**, *68*, 4279.
- (27) Kowalski, K.; Piecuch, P. *J. Chem. Phys.* **2001**, *115*, 2966.
- (28) Kowalski, K.; Hirata, S.; Wloch, M.; Piecuch, P.; Windus, T. L. *J. Chem. Phys.* **2005**, *123*.
- (29) Kowalski, K.; Piecuch, P. *J. Chem. Phys.* **2004**, *120*, 1715.
- (30) Kowalski, K.; Valiev, M. *Int. J. Quantum Chem.* **2008**, *108*, 2178.
- (31) Bartlett, R. J.; Musial, M. *Rev. Mod. Phys.* **2007**, *79*, 291.
- (32) Becke, A. D. *J. Chem. Phys.* **1993**, *98*, 5648.
- (33) Weigend, F.; Ahlrichs, R. *Phys. Chem. Chem. Phys.* **2005**, *7*, 3297.
- (34) Grimme, S.; Waletzke, M. *J. Chem. Phys.* **1999**, *111*, 5645.
- (35) Grein, F. *J. Chem. Phys.* **2007**, *126*.
- (36) Li, S.; Dixon, D. A. *J. Phys. Chem. A* **2008**, *112*, 6646.

- (37) Chen, M.; Dixon, D. A. *Journal of Chemical Theory and Computation* **2013**, *9*, 3189.
- (38) See supplementary material document no. _____ for relevant cluster geometries, tables of excitation energies and orbitals involved in the excitations for monomer and dimer.
- (39) Schafer, A.; Horn, H.; Ahlrichs, R. *J. Chem. Phys.* **1992**, *97*, 2571.
- (40) Balabanov, N. B.; Peterson, K. A. *J. Chem. Phys.* **2005**, *123*.
- (41) Ahlrichs, R.; Bar, M.; Haser, M.; Horn, H.; Kolmel, C. *Chem. Phys. Lett.* **1989**, *162*, 165.
- (42) Lai, P.-W.; Zhang, H.; Rajbhandari, S.; Valeev, E.; Kowalski, K.; Sadayappan, P. In *Proceedings of the international conference on computational science, iccs 2012*; Ali, H., Shi, Y., Khazanchi, D., Lees, M., VanAlbada, G. D., Dongarra, J., Sloot, P. M. A., Eds. 2012; Vol. 9, p 412.
- (43) Valiev, M.; Bylaska, E. J.; Govind, N.; Kowalski, K.; Straatsma, T. P.; Van Dam, H. J. J.; Wang, D.; Nieplocha, J.; Apra, E.; Windus, T. L.; de Jong, W. A. *Comp. Phys. Commun.* **2010**, *181*, 1477.
- (44) Garkusha, I.; Nagy, A.; Guennoun, Z.; Maier, J. P. *Chem. Phys.* **2008**, *353*, 115.
- (45) Wang, H.; Steimle, T. C.; Apetrei, C.; Maier, J. P. *Phys. Chem. Chem. Phys.* **2009**, *11*, 2649.
- (46) Zhuang, X.; Le, A.; Steimle, T. C.; Nagarajan, R.; Gupta, V.; Maier, J. P. *Phys. Chem. Chem. Phys.* **2010**, *12*, 15018.